

# INFLUENCE OF LOADING SEQUENCE AND STRESS RATIO ON FATIGUE DAMAGE ACCUMULATION OF A STRUCTURAL COMPONENT

HÉLDER F. S. G. PEREIRA\*, ABÍLIO M.P. de JESUS\*<sup>§</sup>, ALFREDO S. RIBEIRO\*<sup>§</sup>,  
ANTÓNIO A. FERNANDES\*<sup>‡</sup>

\*UCVE, IDMEC – Pólo FEUP, Rua Dr. Roberto Frias, 4200-465 Porto, Portugal.

<sup>§</sup>University of Trás-os-Montes and Alto Douro, Engineering Department,  
Quinta de Prados, 5001-801 Vila Real, Portugal.

<sup>‡</sup>University of Porto, Faculty of Engineering, Rua Dr. Roberto Frias, 4200-465 Porto, Portugal.  
hfpereira@portugalmail.pt

**ABSTRACT:** This paper presents experimental results about the fatigue damage accumulation behaviour of a structural component made of P355NL1 steel. The structural component is a rectangular double notched plate. Two and multiple alternated constant amplitude block sequences were applied for various combinations of remote stress ranges. Three stress ratios were investigated, namely  $R=0$ ,  $R=0.15$  and  $R=0.3$ . Variable amplitude blocks were also investigated according predefined stress spectra. Constant amplitude data was also generated which is applied for damage calculation purposes. In general, the block loading demonstrates that fatigue damage evolves nonlinearly with the number of loading cycles, function of the load sequence, stress level and stress ratios. Generally, the application of variable amplitude loading suggests an important stress ratio effect on fatigue damage accumulation. In particular, a clear load sequence effect is verified for the two block loading, with null stress ratio. For the other (higher) stress ratios, the load sequence effects are almost negligible; however the damage evolution still is non-linear.

**Keywords:** Fatigue Damage; Stress Ratio; Loading Sequence; Structural Component; P355NL1 steel.

**RESUMO:** Este artigo apresenta resultados experimentais relativos à acumulação de dano de fadiga de um componente estrutural de aço P355NL1. O componente estrutural é uma placa rectangular com duplo entalhe. Foram aplicadas sequências de dois e múltiplos blocos de carga de amplitude constante, para várias combinações de razões de tensão remotas, nomeadamente  $R=0$ ,  $R=0.15$  e  $R=0.3$ . Também foram analisados os efeitos da aplicação de blocos de amplitude variável, aplicados de acordo com um espectro de carga predefinido. Este estudo foi complementado com resultados de ensaios realizados em amplitude constante, os quais serviram para os cálculos de acumulação de dano. Em geral, o carregamento por blocos demonstra que o dano provocado por fadiga apresenta uma evolução não linear com o número de ciclos de carga, sendo esta evolução de dano função da sequência de carga, do nível de tensão e da razão de tensões. Geralmente, a aplicação de carregamentos de amplitude variável indicia um importante efeito da razão de tensões na acumulação de dano por fadiga. Particularmente, é observado um efeito claro da sequência de carga nos carregamentos compostos por dois blocos de carga, com razão de tensões nula. Para as outras razões de tensões (altas), os efeitos da sequência de carga são praticamente desprezáveis; contudo a evolução de dano continua a ser não linear.

**Palavras chave:** Dano à Fadiga; Razão de Tensões; Sequência de Carga; Detalhe Estrutural; Aço P355NL1.

## 1. INTRODUCTION

Structures and components under service conditions are frequently subjected to random or variable amplitude block loading. Different relations [1] have been proposed to calculate the effect of variable amplitude loading conditions. However, these procedures need the identification of many parameters.

In the design of steel structures against fatigue, one of the problems that have attracted increased attention in recent years is the problem of fatigue damage accumulation. Code specifications usually suggest simple rules such as the Palmgren-Miner's linear summation rule which are based on results from constant amplitude fatigue tests. For example, the

fatigue analysis procedures for a spectrum loading, proposed by the EN13445 standard [2] on its Part 3, Clauses 17 and 18 for fatigue design of unfired pressure vessels, are based on the linear cumulative damage concept due to Palmgren and Miner [3]. This type of analysis neglects the load sequential effects that occur during the loading history.

Due to its simplicity, the Palmgren-Miner's linear damage rule still is widely used for design purposes, in spite of its limitations. Its major limitation is the lack of consideration of the effect of the loading sequence; that is the effect of the interaction between higher to lower stress levels or vice-versa. Most of metallic materials exhibit more complex behaviours than modelled by a linear damage rule. It has been verified that metallic materials exhibit highly nonlinear fatigue damage evolution with load dependency [4-8]. The last two characteristics yield a nonlinear damage accumulation behaviour that accounts for loading sequential effects. Thus, depending on load history, the Palmgren-Miner's rule can underestimate or overestimate the fatigue damage.

Several attempts have been done to propose more reliable fatigue damage rules. Manson [9], Fatemi [1] and Schijve [10] present a comprehensive review about fatigue damage models. However, the new propositions are limited to very specific conditions (e.g. certain loading sequences, materials) hindering the adoption of those rules in current design practices.

The main goal of this paper is to report experimental evidence about the fatigue damage accumulation behaviour of a structural component made of P355NL1 steel subjected either to constant and variable amplitude block loading, applied in the form of a controlled remote stress.

## 2. CUMULATIVE DAMAGE MODELS

### 2.1. Linear model

Fatigue life prediction under constant amplitude block loading is often based on the linear Palmgren-Miner's damage rule [3]. According to this rule the fatigue damage can be evaluated as follows:

$$D = \sum_{i=1}^k \frac{n_i}{N_i} \quad (1)$$

where  $D$  is the fatigue damage,  $k$  is the number of constant amplitude blocks,  $n_i$  is the number of load cycles applied during the block  $i$  characterized by a maximum stress  $\sigma_{max,i}$ , and  $N_i$  is the number of failure cycles that would result for the solely application of the loading conditions ( $\sigma_{max,i}$ ) of block  $i$ . The failure is expected to occur when damage reaches the unity,  $D=1$ . The number of cycles to failure,  $N_i$ , is evaluated using constant amplitude fatigue data, by means of the S-N curve. The S-N curve can be written in the following general form [11]:

$$(\sigma_{max})^m N = C \quad (2)$$

where  $C$  and  $m$  are material constants and  $\sigma_{max}$  is the maximum stress of the cycle. Replacing equation 2 into equation 1 results the following alternative form of the damage equation:

$$D = \frac{1}{C} \sum_{i=1}^k n_i (\sigma_{max,i})^m \quad (3)$$

Using the Palmgren-Miner's concept it is possible to define, for a block loading, an equivalent maximum stress,  $\sigma_{max,eq}$ , as a stress that induces the same damage when applied for the same total number of cycles of the block loading:

$$\sigma_{max,eq} = \left[ \frac{\sum_{i=1}^k n_i (\sigma_{max,i})^m}{\sum_{i=1}^k n_i} \right]^{1/m} \quad (4)$$

The two block loading defined by one high and one low stress amplitude blocks, applied respectively during  $n_H$  and  $n_L$  cycles deserves special interest in this research. Using the Palmgren-Miner's linear relation it is possible to write the following damage relation for the two-block loading:

$$D = \frac{n_H}{N_H} + \frac{n_L}{N_L} \leq 1 \quad (5)$$

This relation is not sensible to the loading sequence. For two block loading, relation (4) becomes:

$$\sigma_{max,eq} = \left[ \frac{n_H (\sigma_{max,H})^m + n_L (\sigma_{max,L})^m}{n_H + n_L} \right]^{1/m} \quad (6)$$

### 2.2. Non-Linear model

Some authors (ex. Marco and Starkey [13]) suggested the replacement of the Palmgren-Miner's rule by the following non-linear relation:

$$D = \left( \frac{n}{N} \right)^\alpha \quad (7)$$

where  $\alpha$  is a function of the applied load, to be identified on the basis of experimental data. This relation models a non-linear damage evolution with the number of loading cycles, as illustrated schematically in Fig. 1 for two block loading. The load dependency of  $\alpha$  allows the description of the load sequential effects also illustrated in Fig. 1. Based on Fig. 1, it is possible to write the following damage relations, respectively for High-Low and Low-High block loading sequences:

High-Low:

$$D_A = D_B \Rightarrow \left( \frac{n_H}{N_H} \right)^{\alpha_H} = \left( 1 - \frac{n_L}{N_L} \right)^{\alpha_L} \Leftrightarrow \frac{n_L}{N_L} = 1 - \left( \frac{n_H}{N_H} \right)^{\frac{\alpha_H}{\alpha_L}} \quad (8)$$

Low-High:

$$D_A = D_B \Rightarrow \left( \frac{n_L}{N_L} \right)^{\alpha_L} = \left( 1 - \frac{n_H}{N_H} \right)^{\alpha_H} \Leftrightarrow \frac{n_H}{N_H} = 1 - \left( \frac{n_L}{N_L} \right)^{\frac{\alpha_L}{\alpha_H}} \quad (9)$$

The absolute values of  $\alpha_L$  and  $\alpha_H$  are not possible to extract using the available data. For this purpose, damage measurements would be required in order to be used with relation (7) [4].

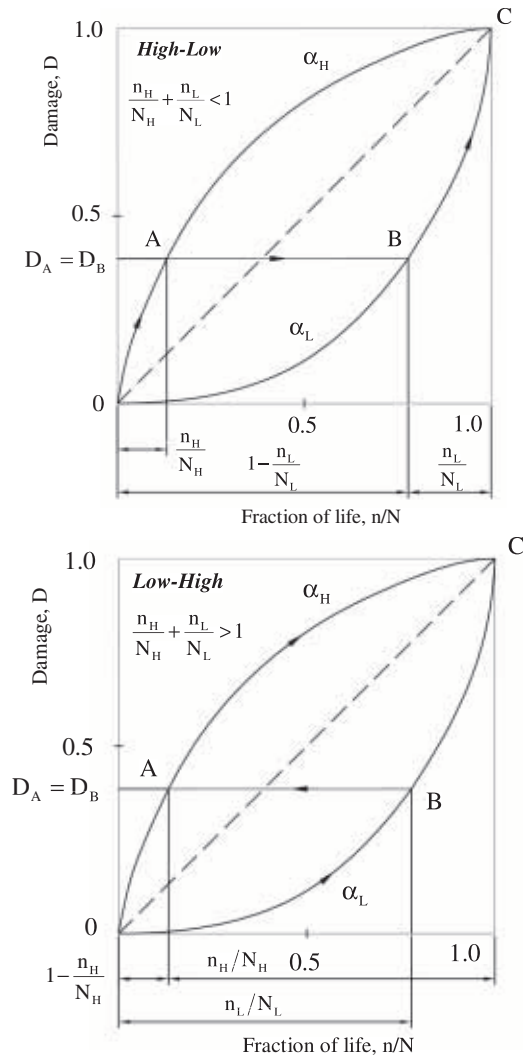


**Fig. 1.** Illustration of the non-linear damage evolution and load sequential effects for two block loading.

**3. EXPERIMENTAL PROGRAM**

The present research is based on a comprehensive experimental program which included fatigue tests of notched specimens machined from 3140x2000x5.1mm<sup>3</sup> P355NL1 steel sheets. The P355NL1 steel is intended for pressure vessel applications and is a normalized fine grain low alloy carbon steel. The chemical composition and mechanical properties of the material are given in Tables 1 and 2, respectively. Specimens are double notched rectangles extracted in the rolling direction of the steel sheets. The geometry of the specimens is illustrated in Fig. 2. Peterson [13] specify for this geometry an elastic stress concentration factor,  $K_t=2.17$ . The dimensions pointed out in the figure were verified for all specimens prior testing. Both lateral faces of the specimens were polished using the

following sequence of sandpapers numbers: 320, 500, 800, 1000, 1200 and 2500.

All fatigue tests were conducted in an INSTRON 8801 servo-hydraulic machine, rated to 100 kN. These tests were performed under remote uniaxial stress-controlled conditions according to the stress ratios,  $R=0$ ,  $R=0.15$  and  $R=0.3$ . Also tests with variable stress ratios were carried out. A sinusoidal waveform was applied in all tests.

Constant amplitude tests were carried out in order to derive the S-N curve for the component. Also two and multiple alternated constant amplitude block loading tests were performed to assess the damage accumulation behaviour of the component. High-Low (H-L), Low-High (L-H), H-L-H-L(...) and L-H-L-H(...) block sequences were investigated. Figure 3 illustrates the investigated constant amplitude block loading sequences. For two block loading, while the first block is applied during a predefined number of cycles, the second block is applied until the failure of the specimen. Finally, tests with variable amplitude block loading, following a Gaussian distribution, were applied as illustrated in Fig. 4.

**Table 1.** Chemical composition of the P355NL1 steel (% weight).

C	Si	Mn	P	S	Al	Mo
0.133	0.35	1.38	0.014	0.0016	0.03	0.001
Nb	Ni	Ti	V	Cu	Cr	
0.025	0.148	0.016	0.002	0.137	0.025	

**Table 2.** Mechanical properties of the P355NL1 steel [6].

Ultimate tensile strength, $\sigma_{UTS}$ [MPa]	568
Monotonic yield strength, $\sigma_y$ [MPa]	418
Young modulus, $E$ [GPa]	205.2
Poisson's coefficient, $\nu$	0.275
Cyclic hardening coefficient, $K'$ [MPa]	777
Cyclic hardening exponent, $n'$ [-]	0.1068
Fatigue strength coefficient, $\sigma_f'$ [MPa]	840.5
Fatigue strength exponent, $b$ [-]	-0.,0808
Fatigue ductility coefficient, $\epsilon_f'$ [-]	0.,3034
Fatigue ductility exponent, $c$ [-]	-0.6016

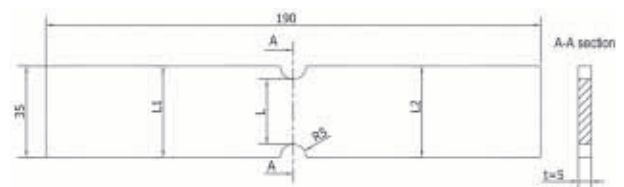


**Fig. 2.** Geometry of the specimen (dimensions in mm).

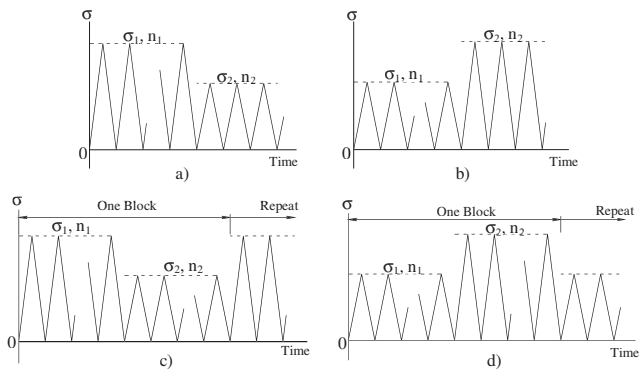


**Fig. 3.** Investigated constant amplitude block loading,  $R=0$ : a) H-L sequence; b) L-H sequence; c) H-L-H-L(...) sequence and d) L-H-L-H(...) sequence.

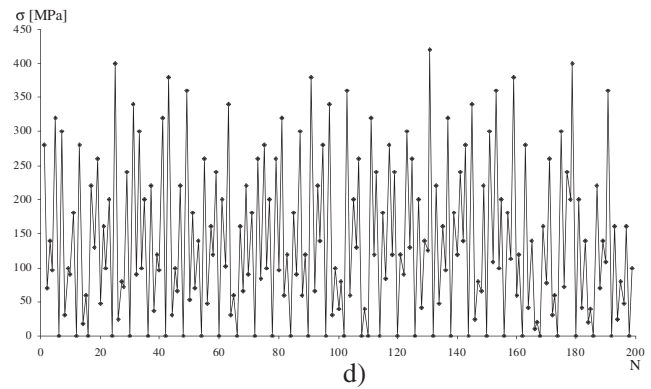


**Fig. 4.** Example of investigated variable amplitude block loading: a) L-H sequence with  $R=0$ ; b) H-L sequence with  $R=0$ ; c) L-H-L sequence with  $R=0.3$ ; d) random sequence.

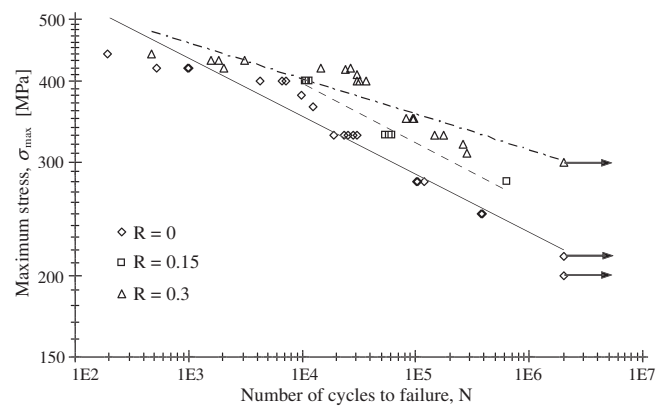
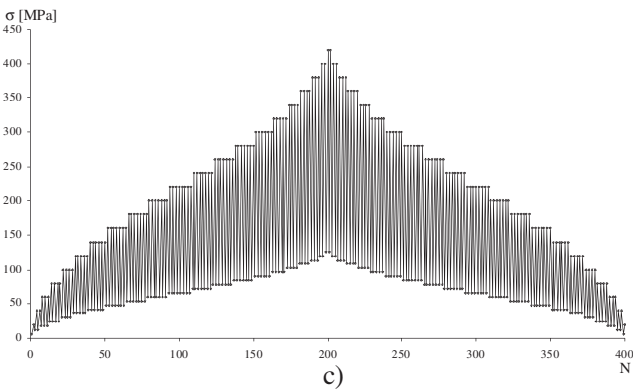
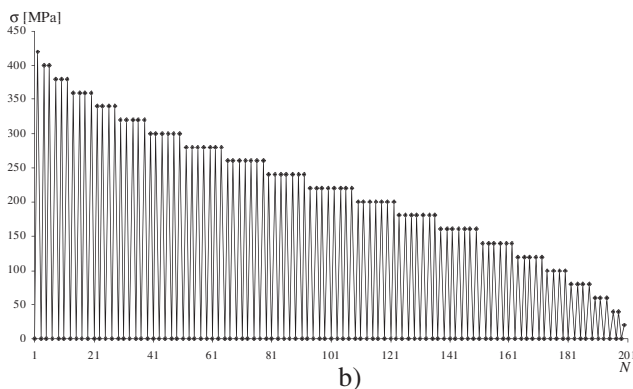
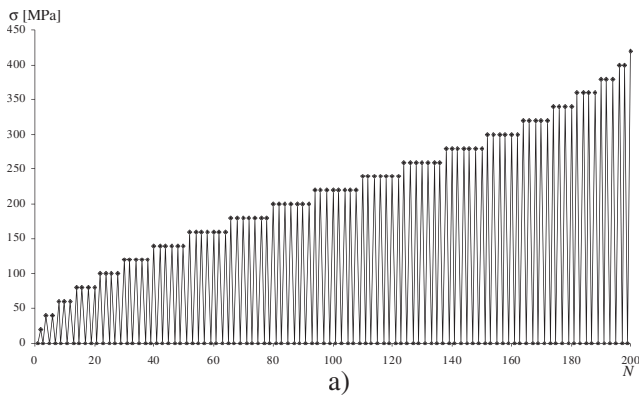


**Fig. 5.** S-N curves for the structural component.

## 4. EXPERIMENTAL RESULTS AND DISCUSSION

### 4.1. Constant amplitude loading

The S-N curves obtained for the structural component under constant stress amplitude for stress ratios  $R=0$ ,  $R=0.15$  and  $R=0.3$  are plotted in Fig. 5. The analysis of the figure is conclusive relative to the stress ratio effect. For the same maximum cyclic stress, the fatigue life increases as the stress ratio increases; conversely, for the same stress amplitude the increasing of the stress ratio reduces the fatigue life. Table 3 summarizes the constants  $C$  and  $m$  of the S-N curves defined according to equation (2). The coefficient of determination,  $R^2$ , is also included. Finally, the table includes the fatigue endurance limit,  $\sigma_{f0}$ , in the form of a cyclic maximum stress.

**Table 3.** S-N curves parameters according to equation (2) [8].

$R$	$m$	$C$	$R^2$	$\sigma_{f0}$ [MPa]
0	11.16	2.73E+32	0.9309	200
0.15	10.92	2.39E+32	0.9688	-
0.3	18.35	6.39E+51	0.8295	300

## 4.2. Variable amplitude loading

### 4.2.1. Constant amplitude block loading

Constant amplitude blocks were applied, namely two and multiple alternated blocks. The investigated sequences were High-Low (H-L) and Low-High (L-H), for two block loading, and H-L-H-L(...) and L-H-L-H(...), for multiple alternated block loading. Three stress ratios were investigated, namely  $R=0$ ,  $R=0.15$  and  $R=0.3$ .

The block loading data was transformed into an equivalent constant amplitude data, using the concept of maximum equivalent stress, defined by equation (4). The resulting data is compared with the constant amplitude data. Results are plotted in Figs. 6 and 7 for the stress ratios,  $R=0$ ,  $R=0.15$  and  $R=0.3$  and for H-L and L-H block sequences and in Figs. 8a) and 8b) for the stress ratios,  $R=0$  and  $R=0.3$  and for H-L-H-L(...) and L-H-L-H(...) sequences, respectively. The represented solid line in the referred figures corresponds to the mean S-N curves already plotted in Fig. 5. According to these figures it seems that the concept of equivalent stress, formulated in the Palmgren-Miner's framework, allows a fair description of the block loading data, using information from constant amplitude tests. In fact the block loading data overlay the constant amplitude data. This information may be, however, apparent as can be verified by a more refined analysis described below.

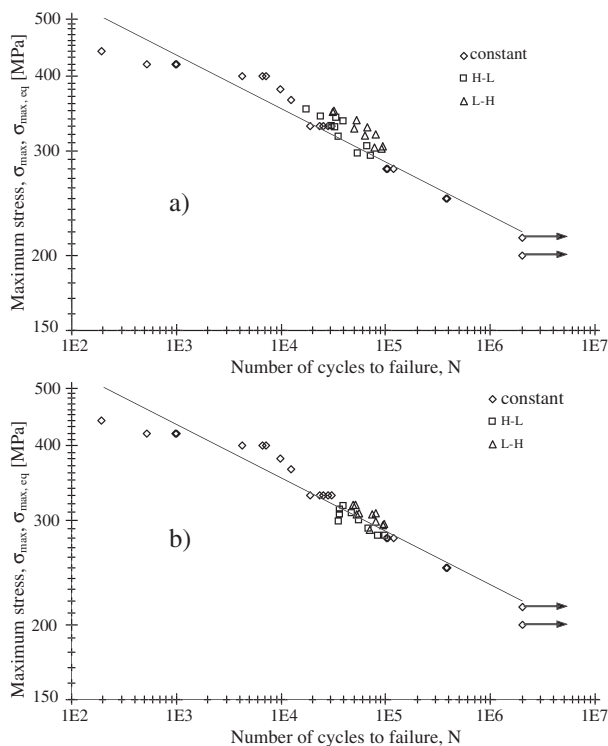


**Fig. 6.** Comparison between constant and block loading data. H-L and L-H sequences ( $R=0$ ): a) defined by 280 and 400 MPa stress ranges; b) defined by 280 and 330 MPa stress ranges.

Figures 9, 10 and 11 propose an alternative representation for the block loading data. The fractions of lives at higher stress amplitudes,  $n_H/N_H$ , are plotted against the fraction of lives at lower stress amplitudes,  $n_L/N_L$ . All figures include the linear Palmgren-Miner's curve for comparison purposes.

It is clear, by the analyses of the figures, that the structural component does not follow the linear damage model. The fatigue damage evolves nonlinearly with the number of cycles. For  $R=0$  (see Figs. 9a) and 9b)) the fatigue damage is also a function of the loading as defined by relations (8)-(9) and the loading sequential effects are clearly visible. On effect, for the H-L loading sequences, the summations of the fractions of lives are lower than unity; for the L-H sequences the summations of the fractions of lives are higher than unity. The best fit of experimental data for  $R=0$  resulted the damage exponent ratios of  $\alpha_L/\alpha_H=2.22$  and  $\alpha_H/\alpha_L=0.45$ , for the combination of 280 and 400 MPa stress ranges, and  $\alpha_L/\alpha_H=2.07$  and  $\alpha_H/\alpha_L=0.48$ , for the combination of 280 and 330 MPa stress ranges. These damage exponent ratios are consistent with the values obtained for the P355NL1 steel, with respect to the loading sequential effects [5, 7].

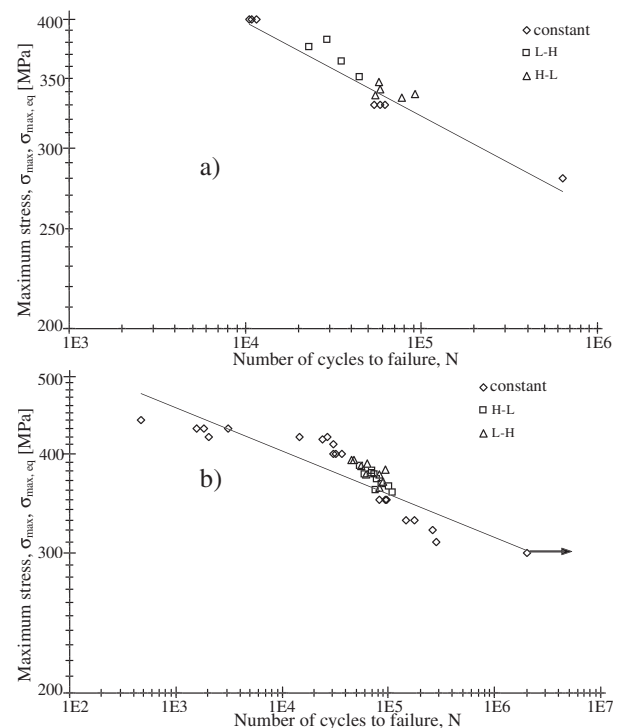


**Fig. 7.** Comparison between constant and block loading data. H-L and L-H sequences: a) defined by 280.5 and 340 MPa stress ranges ( $R=0.15$ ); defined by 245 and 280 MPa stress ranges ( $R=0.3$ ).

Surprisingly, there is an important stress ratio influence on loading sequential effects. For  $R=0.15$  and  $R=0.3$  there is no appreciable loading sequential effects on damage accumulation, as illustrated by Figs. 10a) and 10b). The damage relation (7) fails to predict this behaviour. It seems that the damage exponent  $\alpha$  is no longer a load function. For these two stress ratios, the Palmgren-Miner's linear relation seems to be conservative, since all experimental failure data points lay above it.

For multiple block loading, Figs. 11a) and 11b) do not show any sensibility of the component to the loading sequence. For multiple block loading with  $R=0$  the Palmgren-Miner's linear relation is essentially non conservative, but for  $R=0.3$  the Palmgren-Miner's linear relation is significantly conservative.

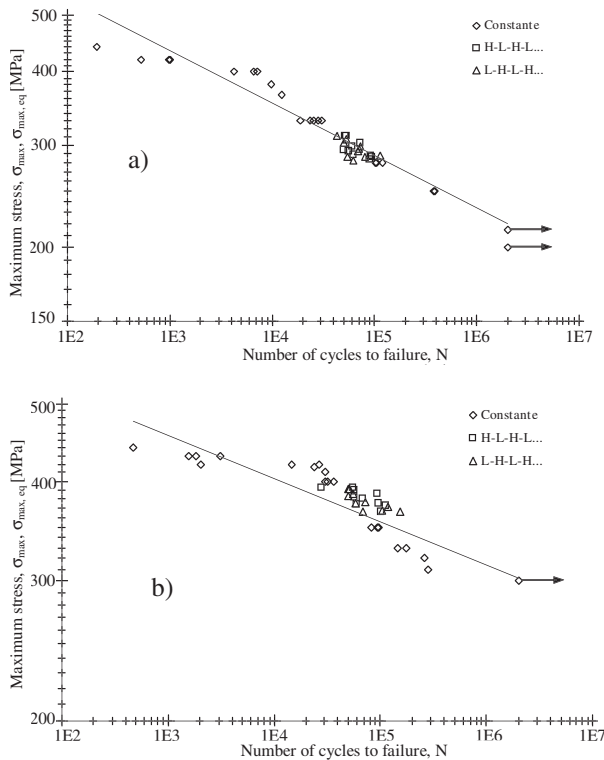


**Fig. 8.** Comparison between constant and block loading data. H-L-H-L(...) and L-H-L-H(...) sequences: a) defined by 330 and 280 MPa stress ranges ( $R=0$ ); defined by 245 and 280 MPa stress ranges ( $R=0.3$ ).

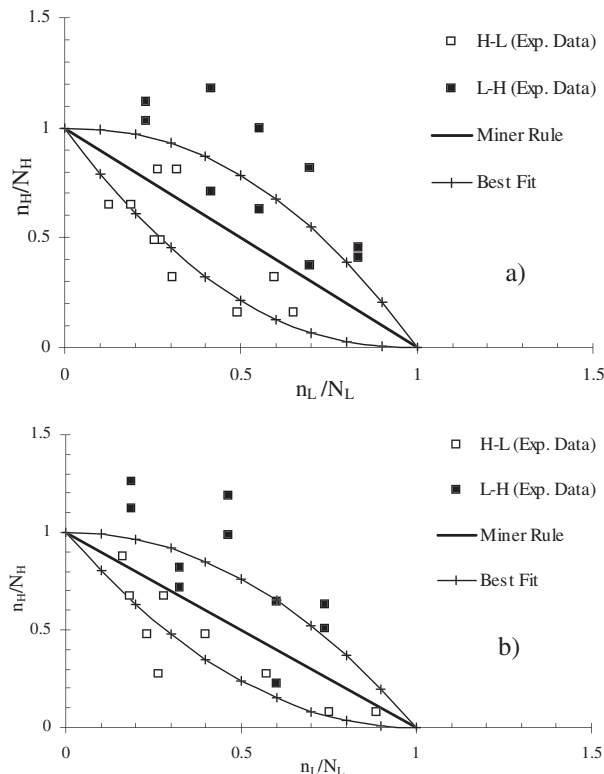


**Fig. 9.** Fatigue data for two block loading: a) defined by 280 and 400 MPa stress ranges ( $R=0$ ); b) defined by 280 and 330 MPa stress ranges ( $R=0$ ).

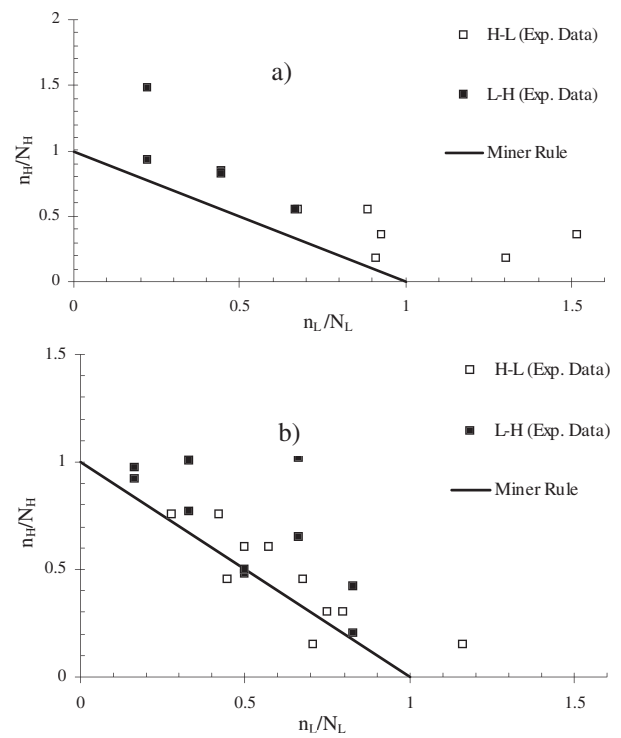


**Fig. 10.** Fatigue data for two block loading: a) defined by 280.5 and 340 MPa stress ranges ( $R=0.15$ ); defined by 245 and 280 MPa stress ranges ( $R=0.3$ ).

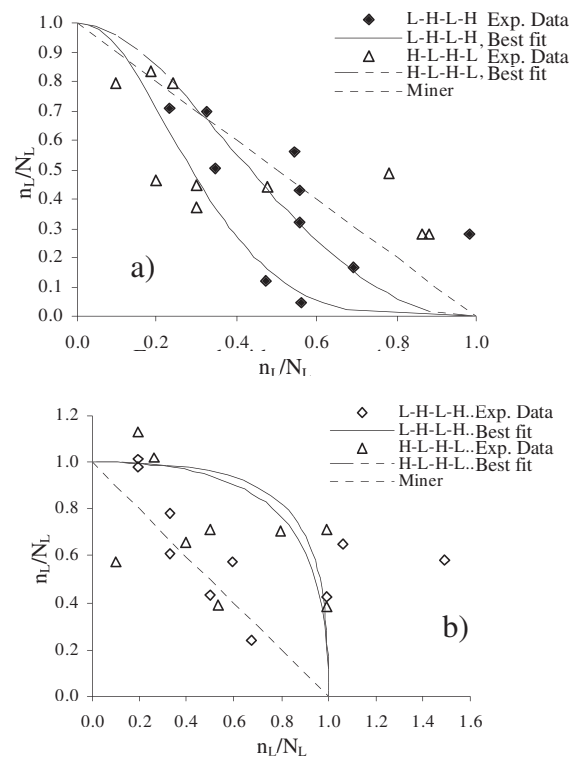


**Fig. 11.** Fatigue data for multiple block loading: a) defined by 330 and 280 MPa stress ranges ( $R=0$ ); defined by 245 and 280 MPa stress ranges ( $R=0.3$ ).

#### 4.2.2. Variable amplitude block loading

The variable amplitude block loading consisted on blocks composed by continuously increasing/decreasing constant amplitude blocks of small duration (see Figs. 4a), 4b) and 4c)) or random loading (see Fig. 4d)). In any case the individual cycles followed a Gaussian distribution. Stress spectra composed by individual cycles of  $R=0$ ,  $R=0.3$  and random were tested. The sequences used were H-L, L-H, L-H-L and random. For those blocks with non null stress ratio, the individual stress cycles were evaluated applying the FATVEN code [14], which is based on reservoir cycle counting method [2]. Figure 12 illustrates a calculation example.

For the variable amplitude block loading, damage calculations, based on cycle ratio summations, as specified by the linear model, were evaluated and results are presented in Tables 4 to 6. A general trend is observed – the cycle ratios summations are greater than unity. For random sequences the cycle ratios summations are near to unity. Thus, the linear model would produce conservative predictions. Also, some results are consistent with observations carried out for constant amplitude block loading data.

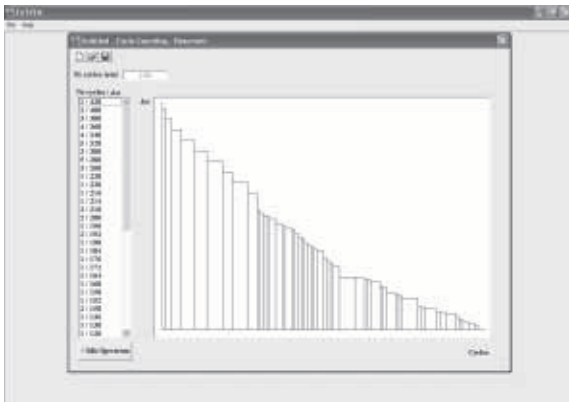


**Fig. 12.** Cycle counting illustration from FATVEN software, random loading.

**Table 4.** Damage calculations for the variable amplitude block loading tests with  $R=0$ .

$\Delta\sigma_{max}$ (MPa)	Sequence	Average damage summation (Miner's Rule)
420	H-L	1.0915
420	L-H	0.8413
420	L-H-L	1.2380
420	Random	0.9157

**Table 5.** Damage calculations for the variable amplitude block loading tests with  $R=0.3$ .

$\Delta\sigma_{max}$ (MPa)	Sequence	Average damage summation (Miner's Rule)
420	H-L	1.485
420	L-H	1.476
420	L-H-L	2.329
420	Random	0.741

**Table 6.** Damage calculations for the variable amplitude block loading tests with random sequences

$\Delta\sigma_{max}$ (MPa)	Sequence	Average damage Summation (Miner's Rule)
420	Random	1.139
420	Random	0.852

#### 4. CONCLUDING REMARKS

This paper discussed the fatigue damage behaviour of a structural detail made of P355NL1 steel under block loading. The block loading was defined by two and multiple alternate constant amplitude blocks. Also variable amplitude blocks were defined by gradually increasing/decreasing small blocks or by random loading. Also, constant amplitude fatigue data was presented for comparison purposes. Three stress ratios were analyzed, namely  $R=0$ ,  $R=0.15$  and  $R=0.3$ .

It was observed for  $R=0$  a damage behaviour compatible with a non-linear damage evolution with the cycles and dependent on loading. This behaviour is responsible for a non-linear damage summation with loading sequential effects.

For  $R=0.15$  and  $R=0.3$  the structural component did not exhibit loading sequential effects on fatigue damage summation. For these two latter stress ratios the Palmgren-Miner's relation yields safe predictions.

For variable amplitude loading the structural component present in general cycle ratios summation greater than unity.

Significant scatter is observed on experimental data. However, it can be considered usual in variable amplitude loading fatigue tests of components.

#### REFERENCES

- [1] A. Fatemi and L. Yang, *International Journal of Fatigue* **20** (1998) 9.
- [2] European Committee for Standardization - CEN, *EN 13445: Unfired Pressure Vessels*, European Standard, Brussels (2002).
- [3] M.A. Miner, *Journal of Applied Mechanics* **67** (1945) A159.
- [4] A.M.P. de Jesus, A.S. Ribeiro and A.A. Fernandes, *Journal of Pressure Vessel Technology* **127** (2005) 157.
- [5] H.F.G.S. Pereira, A.M.P. de Jesus, A.A. Fernandes and A.S. Ribeiro, *Abstracts of the "5th International Conference on Mechanics and Materials in Design"*, 24-26 July, 2006, Porto, Portugal.
- [6] H.F.G.S. Pereira, A.M.P. de Jesus, A.A. Fernandes and A.S. Ribeiro, *Strain* (doi: 10.1111/j.1475-1305.2007.00389.x), in Press.

- [7] H.F.G.S. Pereira, A.M.P. de Jesus, A.A. Fernandes and A.S. Ribeiro, *Abstracts of the "2007 ASME Pressure Vessels and Piping Division Conference"*, 22-27 July, S. Antonio, Texas, USA.
- [8] H.F.G.S. Pereira, A.M.P. de Jesus, A.A. Fernandes and A.S. Ribeiro, *Abstracts of the "2007 ASME Pressure Vessels and Piping Division Conference"*, 22-27 July, S. Antonio, Texas, USA.
- [9] S.S. Manson and G.R. Halford, *Engineering Fracture Mechanics* **25** (1986) 538.
- [10] J. Schijve, *Materials Science* **39** (1986) 307.
- [11] J. Lemaitre and J.-L. Chaboche, Cambridge University Press, Cambridge, UK, 1990.
- [12] S.M. Marco and W.L. Starkey, *Translations of the ASME* **76** (1954) 627.
- [13] R.E. Peterson, *Metal Fatigue*, G. Sines and J.L. Waisman edition, McGraw-Hill Book Company, Inc., New York (1959) 293.
- [14] H.F.S.G. Pereira, A.M.P. de Jesus, A.A. Fernandes and A.S. Ribeiro, *Proceedings of the "10th Portuguese Conference on Fracture"*, 22-24 Fevereiro 2006, Guimarães, Portugal.